Evaluation of the Crack Behaviour in a Bimetallic Weld

Surender Bhandari[1)], Gérard Mottet[2)] and Vincent Robin[2)]

1) Framatome ANP, Paris La Défense, France
2) Systus International – ESI Group, Lyon, France

ABSTRACT

This paper presents the study on the behaviour of a part-through circumferential crack at the interface of a PWR pressuriser bimetallic weld, under a four-point bending load, taking into account the residual stresses due to fabrication. It was conducted in the framework of an European project called BIMET, where the bimetallic weld was tested under the same loading conditions. Three-dimensional elasto-plastic analyses were made using local as well as global approaches and results are compared with those obtained experimentally.

INTRODUCTION

Within the framework of European BIMET project dealing with the structural integrity of bi-metallic components [1], two pipe models with cracks were manufactured and subjected to a four point bending load until the crack propagated. This report deals with the full computation of the first bending test (BIMET01) using a 3D finite element analysis which takes account of the residual stresses due to fabrication. The aim of this analysis is to predict the fracture initiation at the crack placed in the buttering at 1.15 mm from the interface between the ferritic base material and the austenitic steel. To do this, the void growth model of Rice and Tracey is employed [2]. In order to use this local approach criterion, one has to determine the crack propagation angle to properly orient the elements at the crack tip. In fact, previous unpublished work conducted at Systus International has shown that the void enlargement has to be calculated for these elements reoriented in the crack propagation direction. Thus some pre-analyses are required and undertaken before the elastic-plastic finite element computation of BIMET01 test specimen which constitutes the main part of this report.

All numerical simulations are made with SYSWELD® software in elastic-plasticity [3].

GEOMETRY OF BIMET01 TEST

The geometry of the BIMET01 test specimen consists of a bimetallic pipe, made of four cylindrical sections, called A, B, C1 and C2 as shown in figure 1. The bimetallic weld was manufactured at ENSA in Spain using a

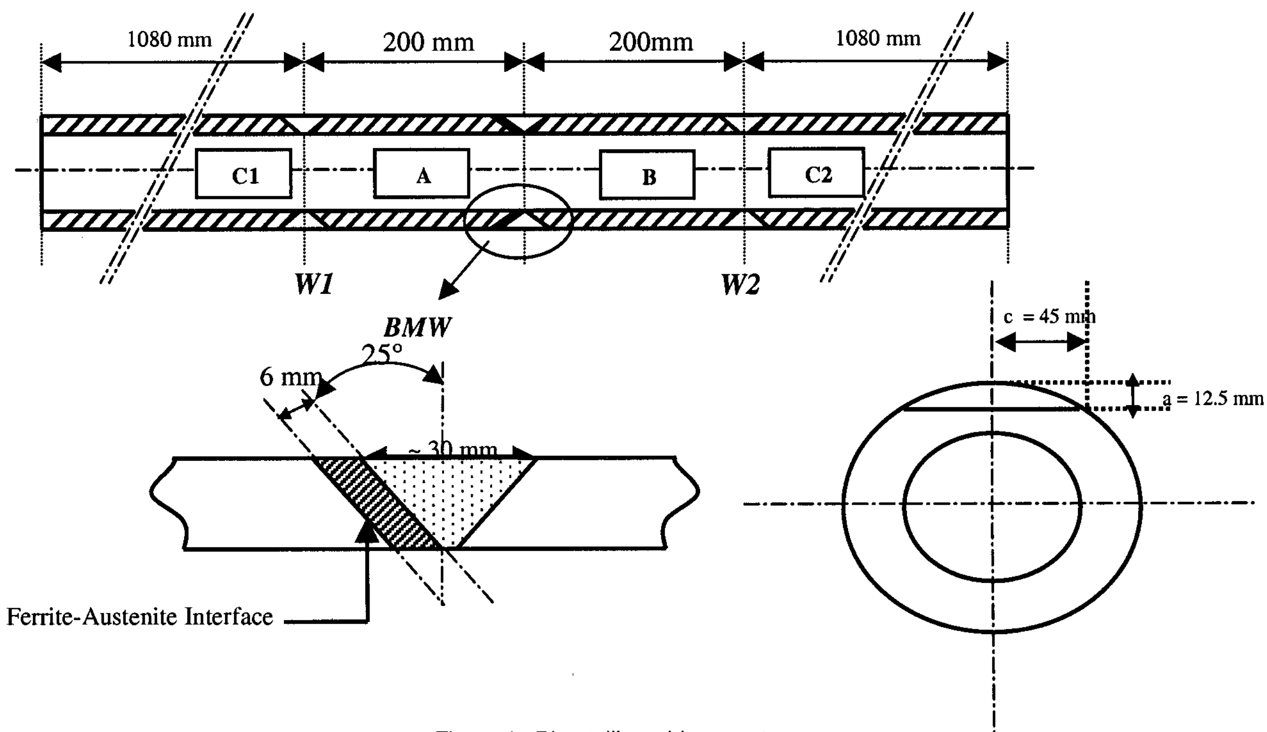

Figure 1 : Bimetallic weld geometry

standard specification for elaboration of a Stainless steel/Ferritic steel weld. In the central part of the tube, section B (made of 304L austenitic steel) is joined to section A (made of A508Cl3 ferritic steel) by a bimetallic weld. At each extremity, two ferritic steel arms C1 and C2 are welded to make the specimen sufficiently long so as to accommodate in the machine for application of the bending moment during the test.

The main dimensions of the structure are show on figure 1. The thickness of the pipe is 25 mm and its external diameter is 168 mm.

The bimetallic welding process consists of two steps :

- buttering of the edge of the ferritic section (about 6 mm thick), first layer of this weld is in 309L austenitic steel and the susequent layers in 308L austenitic steel,
- filling up of the groove with beads in 308L steel.

The defect is realised in the buttering layer with electro-erosion process. It is 1.15 mm from the interface and parallel to it. Its depth reaches half the thickness of the pipe. The crack front projection, in a plane perpendicular to the pipe axis, is straight (see figure 1). The main dimensions of the crack are :
a = 12.5 mm (crack depth projected on a vertical plane)
c = 45 mm (half crack length measured on the pipe section)

EXPERIMENTAL RESULT

From the potential drop measurements made during the test (see figure 2), it was concluded that the initiation moment is situated at a level of about 154 kN.m which corresponds to a ram displacement of 14.7 mm and an applied load of 473 kN.

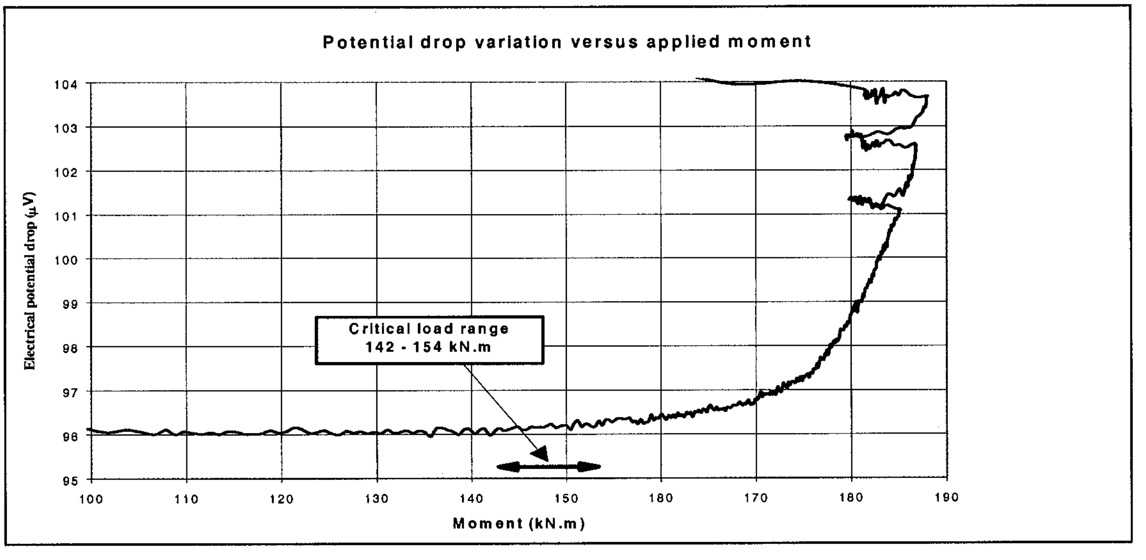

Figure 2: BIMET01 Test - Potential drop measurement at the centre of the crack

FINITE ELEMENT ANALYSIS

Finite Element Modelling

Due to symmetry, only one half of the pipe is modelised. The 3-D finite element model consists of 45859 nodes and 12110 elements. Under-integrated second order elements with 15 or 20 nodes are used. The mesh is refined around the interface and at the crack tip. Care is taken that at the crack tip, the mesh refinement be the same as that used for the cracked Charpy notch specimen. This is because the estimation of local approach parameters has to be done on the same characteristic volume which requires the same element size. The elements used are hexahedrons with sides of 200μm.

Material Properties

The different materials used in the numerical model are :

- A508Cl3 ferritic steel for sections A and C1,
- A508Cl3 HAZ, 2.2mm thick from the interface,
- 309L for the first 2.2mm thick layer of the buttering,
- 308L austenitic steel for the second layer of buttering and groove beads,
- 304L austenitic stainless steel for sections B and C2.

The crack is located in the first layer of buttering made of 309L austenitic steel. It is considered that during the first buttering layer deposit, a heat affected zone appears whose depth is about 2.2 mm. These metallurgical transformations lead to higher mechanical properties. In order to take into account these different material properties in the numerical model, a detailed material characterisation programme was undertaken in the framework of the project, in particular to determine the constitutive laws of the materials involved at room temperature (23°C). Table I gives mean values of measured yield strengths.

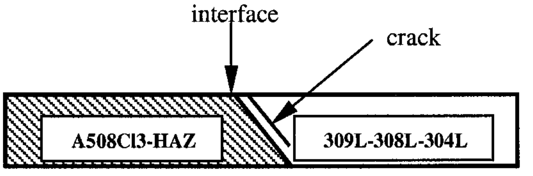

Table I: Material properties used in the numerical model

Material	Yield stress Re 0.2 % (room temperature)	K (Mpa)	n
Base material A508Cl3	516 MPa	1048.4	0.156
Heat-affected zone (HAZ)	725 MPa	1240.5	0.12
309L buttering (first layer)	366 MPa	1301	0.387
308L buttering and groove beads	400 MPa	1011.8	0.234
304L austenitic steel	260 MPa	1065	0.36

Strain hardening due to the restraint of the deposited groove beads is much higher in the inner part of the groove than in the outer part. Nevertheless, for the three-dimensional calculation, the same material properties are considered for the second layer of buttering and the groove beads, in the whole structure.

Stress values induced by W1 and W2 welds are not evaluated because they have no important effect on the behaviour of the bimetallic weld being studied. Furthermore, as the stress peaks occur very close to the interface, only the buttering part properties are significant. Strain hardening is assumed to be isotropic for each material. Constitutive laws have been extrapolated to high plastic strain values based on the relation $\sigma=K.\varepsilon_p^n$. Values of K and n coefficients are also summarised in Table I.

Loading and Boundary Conditions

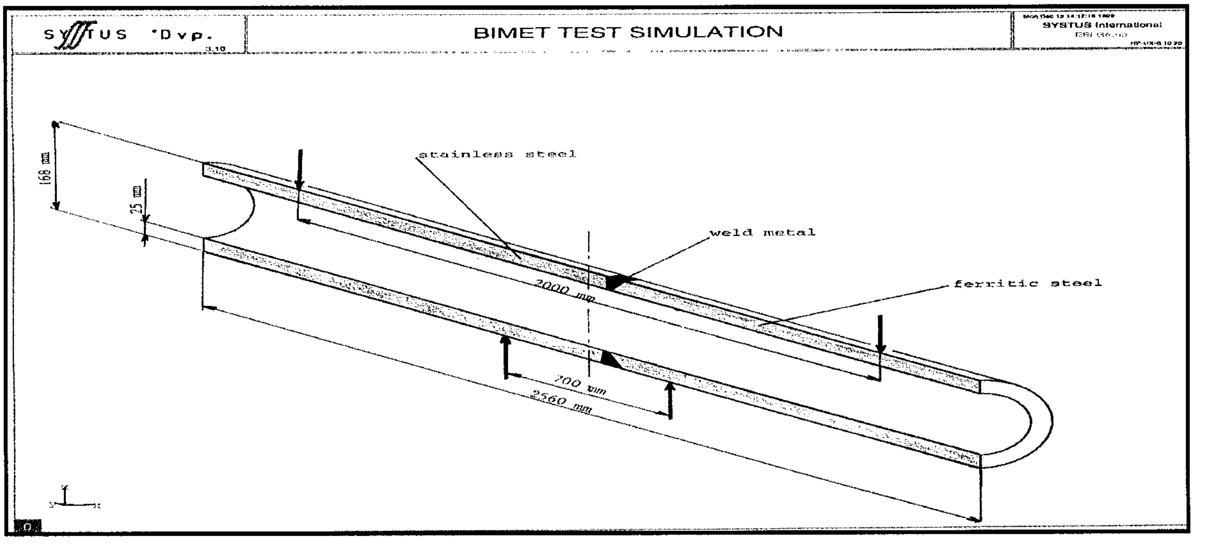

Figure 3: BIMET test simulation

-Heat treatment and defect manufacturing :Residual stresses are induced by welding processes (buttering, groove filling) and stress-relieving heat treatment. The numerical evaluation of residual stresses is made in a simplified way by only simulating the cooling from stress-relieving heat treatment. Stresses are supposed to be negligible at 610°C (stress relieving temperature). During cooling to room temperature, stresses are generated by the difference of thermal expansion coefficients between the ferritic and austenitic steels. This simulation of the cooling process is realised by linking the crack lips together using a special kind of elements. At the end of simulation, these links are broken in order to evaluate the redistribution of residual stresses due to the introduction of the defect.

-Simulation of the bending BIMET01 Test : The four-point bending test configuration is shown on figure 3. In the four-point bending test configuration, the bimetallic weld is placed at the middle of the testing facility so that the crack is submitted to a pure bending moment loading. Two node lines placed 2000 mm apart are restrained from movement in the vertical direction. At the two node lines positioned 700 mm apart, an equal vertical displacement (UZ) is imposed to simulate the ram displacement that results in the application of the bending moment to the pipe. Nodes on the plane of symmetry are constrained from displacing in the direction normal to that plane (direction OX).

ELASTIC ANALYSIS

Stress Intensity Factors

The aim of this elastic analysis is to evaluate which fracture mode initiates the crack propagation behaviour under the four-point bending load applied to the pipe. For such an analysis no residual stresses are considered.

Figure 4 shows the variation of stress intensity factors (K_I, K_{II}, K_{III}) along the crack front for a ram displacement of 1 mm. J-integral can be calculated using these values as follows:

$$J = \frac{K_I^2 + K_{II}^2}{E}(1-\upsilon^2) + \frac{K_{III}^2}{E}(1+\nu) \quad (1)$$

This formula is valid only when there is no crack deviation.

For 1 mm of ram displacement, stress intensity factors in the plane of symmetry are given by:

$K_I = 306.25$ Mpa/mm$^{1/2}$; $K_{II} = 62.60$ Mpa/mm$^{1/2}$; $K_{III} = 0$ Mpa/mm$^{1/2}$ which leads to:

$J = 0.4513$ KJ/m^2 with $E = 197000$ MPa and $\upsilon = 0.3$

This J computation using K values is in good agreement (within 6%) with energy release rate G estimated by θ-method which gives J=G=0.423 KJ/m^2.

Prediction of crack propagation angle

The angle of the crack propagation can be estimated by the maximum circumferential stress method that is detailed below. The circumferential stress value is given by the following equation :

$$\sigma_{\theta\theta} = \frac{\cos^2\left(\frac{\alpha}{2}\right)\left(K_I \cos\left(\frac{\alpha}{2}\right) - 3K_{II}\sin\left(\frac{\alpha}{2}\right)\right)}{\sqrt{2\pi d}} \quad (2)$$

where d is the distance between the point where the stress value is calculated and the tip of the crack, and α is the crack propagation angle. Thus $\sigma_{\theta\theta}$ is maximum when

$$K_I \sin\alpha_o + K_{II}(3\cos\alpha_o - 1) = 0 \quad (3)$$

that gives the following angle of propagation :

$$\alpha_o = 2Arctg\left(\frac{K_I - \sqrt{K_I^2 + 8K_{II}^2}}{4K_{II}}\right) \quad (4)$$

This method was proposed by Erdogan and Sih [4] for plates. In order to use this, values of SIF have to be considered in the plane of symmetry in order to transpose these to a 2-D configuration. Thus, using the previous values of KI and KII, the propagation angle of the crack is about 22° with respect to the plane of the defect, that is corresponding almost to the vertical axis. For the ease of computation, however, for elastic-plastic analysis, the elements at the crack front are reoriented along the vertical axis which makes an angle of 25° with the defect.

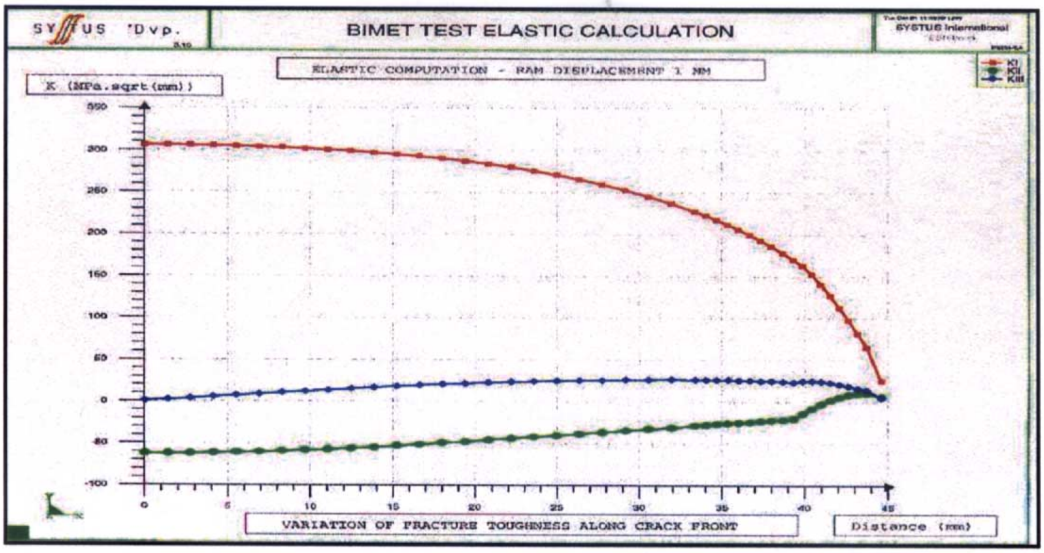

Figure 4: Variation of stress intensity factors along the crack front

ELASTIC PLASTIC ANALYSIS

Geometrical non-linearity is taken into account using large displacement and large strain Lagrange formulation. The maximum ram displacement imposed is 30 mm.

Results

Results have been obtained with respect to the force and the bending moment applied to the structure, and the CMOD (Crack Mouth Opening Displacement) for several values of the ram displacement. Due to limitation of space, only some of the figures will be presented here. Figure 5 (left) shows the numerically computed bending moment with respect to the ram displacement, compared with the corresponding result obtained experimentally. Figure 5 (right) shows the evolution of bending moment with respect to the crack mouth opening displacement (CMOD). In both of these figures, one notices that for the first steps of calculation, the experimental and numerical curves are in good agreement. However, as the ram displacement reaches a value of 9mm, the structure rigidity given by the numerical simulation decreases more rapidly. This may be due to the low yield stress of the austenitic section B made of 304L, which leads to large plastic deformations in this section, as observed in the numerical solution. It was therefore concluded that the actual 304L material properties must be higher than those used in the numerical simulation.

To get an idea of the deformation behaviour of the structure, figure 6 shows the displacement field on the deformed shape for the last calculated step i.e. for ram displacement of 30 mm.

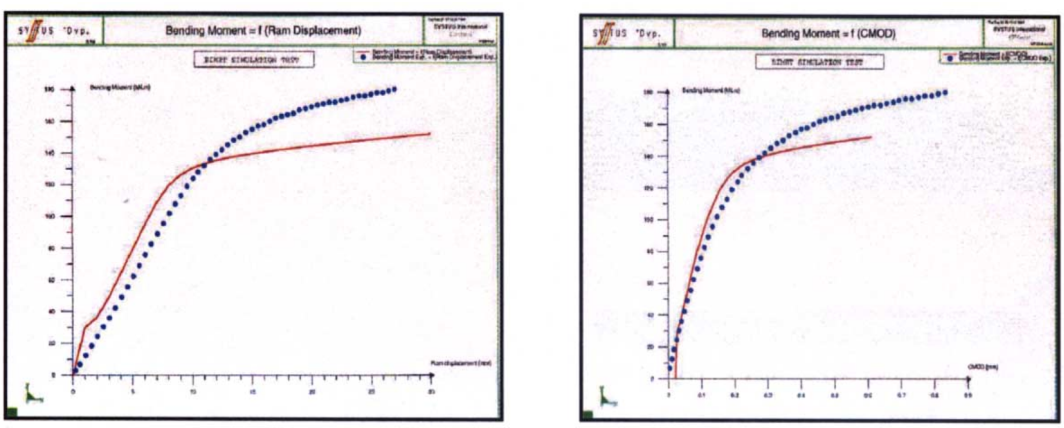

Figure 5: Evolution of applied bending moment with respect to ram displacement/CMOD

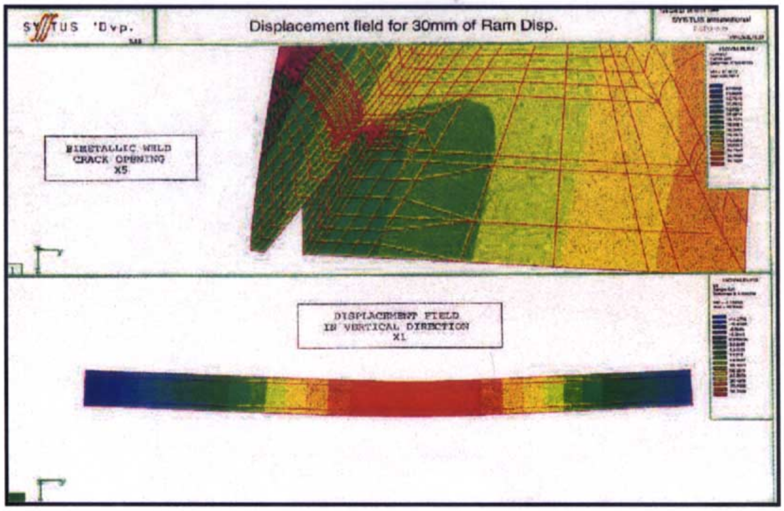

Figure 6: Numerical deformation behaviour of the Structure at 30 mm Ram displacement

Void growth model

The void growth model as given by Rice and Tracey [2] has been calibrated on the results of Charpy notched specimens tested on the first buttering layer, in the framework of the project. The values of the estimated parameters are given as follows:

(R/Ro)c	J_{IC} (kJ/m²)	dJ/da (MPa)
1.33	135	185

where R is the current radius of the void during growth and Ro is the Initial void radius.

Prediction of the fracture initiation

Figure 7 shows the variation of R/Ro with respect to the applied bending moment. The critical value of R/Ro (1.33) is reached for a bending moment of approximately 149 kN.m. This value is somewhat lower than that obtained experimentally (154 kN.m). The numerical simulation tends to over-predict the fracture initiation. From figure 5, one can observe that this moment corresponds to a CMOD of 0.49mm. Using figure 8, which gives the relation between CMOD and the J-Integral, the predicted value of J for fracture initiation is given by 133 kJ/m². Table II shows the comparison of numerical predictions of fracture initiation at the middle of crack front using finite element analysis results, with the first estimate based on electrical potential drop measurements obtained during the test.

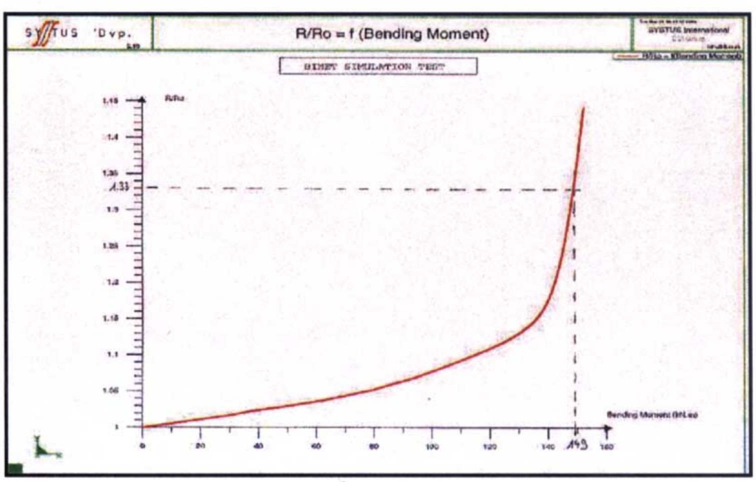

Figure 7: Evolution of R/RO with respect to the applied Bending Moment

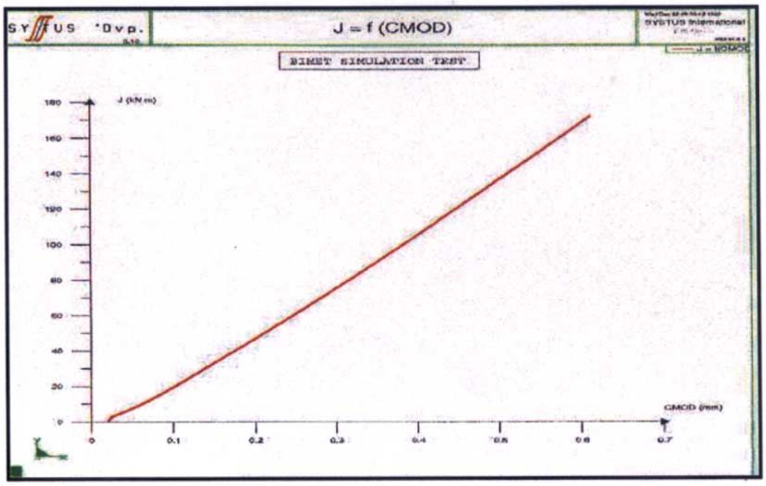

Figure 8: Relation between J-Integral and the Crack Mouth Opening Displacement

Table II: Comparison between numerical prediction and experimental estimate of fracture initiation

	Experiment	Numerical simulation
Ram displacement (mm)	14.7	~25
Bending Moment (kN.m)	154	149
CMOD (mm)	0.341	0.490
J (kJ/m^2)	-	133

CONCLUSIONS

The BIMET01 test has been modelled using elastic-plastic three-dimensional finite element analysis with large strain assumption. The comparison between experimental results and the numerical analysis is quite good. However, for large ram displacement values, numerical results deviate from the experimental values. This could probably be explained by the large plastic deformation of austenitic section B developed during the numerical simulation, which leads to the conclusion that the 304L material properties might be higher than those used in the numerical simulation.

The predicted results concerning the bending moment to fracture initiation are in good agreement with the experimental value (149kN.m for the simulation compared with 154kN.m during the test). Indeed, this moment does not depend on the large plastic strains in the 304L section, and it is directly applied to load the crack.

Good agreement is also observed between R/Ro-J curves for both BIMET01 test and Charpy specimen simulation (see figure 9) since J1c corresponding to the R/Ro critical value of 1.33 at predicted crack initiation (133 kJ/m^2), is quite similar to the value estimated with the simulation of the Charpy specimen test (135 kJ/m^2).

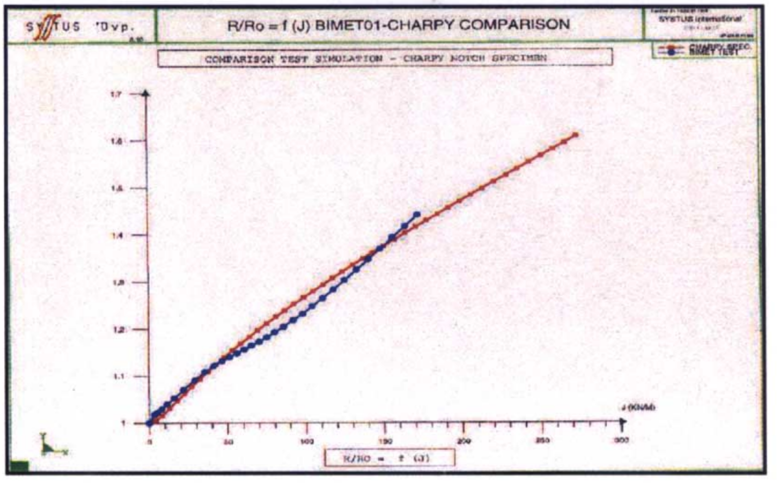

Figure 9 Relation between R/Ro and J-Integral for BIMET01 simulation and CHARPY test specimen

ACKNOWLEDGEMENTS

The authors wish to acknowledge the financial support from DG XII of the European Commission, under the Euratom Fourth Framework Programme 1994-1998: 'Nuclear Fission Safety'.

REFERENCES

[1] Faidy, C., *BIMET:* "Structural Integrity of Bi-metallic Components" - Program Status, *ASME PVP Vol. 410-1, Assessment Methodologies for preventing failure, Volume 1,* ASME,New York, 2000.
[2] Rice, J.R. and Tracey, D.M., "On the ductile enlargement of voids in triaxial stress fields", Journal of Mechanics and Physics of Solids, volume 17, 1969.
[3] SYSWELD® , *Reference manual,* Systus International – ESI Group.
[4] Erdogan, F. Sih, G.C. "On the crack extension in plates under tension loading and transverse shear", Trans. ASME Journal of Basic Engineering, 85D, 519-525, 1963.